IJCRT.ORG ISSN : 2320-2882

INTERNATIONAL JOURNAL OF CREATIVE RESEARCH THOUGHTS (IJCRT)

An International Open Access, Peer-reviewed, Refereed Journal

MPPT For Power Quality Improvement Through Grid Integration Of Renewable Energy Sources

[1] Rakesh kumar Ghasal, [2]Balwant Singh Kuldeep, [3]Rahul Kumar

[1]M.Tech Scholor, [2]Assistant Professor, [3]Assistant Professor

[1]Department of Electrical Engineering,

[1]Sri Balaji College of Engineering and Technology, jaipur, Rajasthan, India

Abstract: Maximizing PowerPoint Tracking (MPPT) techniques are crucial for optimizing the performance of renewable energy sources (RES) integrated with the grid. This paper investigates the application of MPPT algorithms to enhance power quality during the grid integration of RES. The study focuses on photovoltaic (PV) systems and wind turbines, which are prominent RES due to their abundance and environmental benefits. The primary objective is to develop and evaluate advanced MPPT algorithms capable of improving the energy extraction efficiency and stability of RES under varying environmental conditions. Special attention is given to the mitigation of grid disturbances caused by fluctuating RES output, such as voltage fluctuations and harmonics.

The proposed MPPT strategies are implemented and validated through simulation studies using MATLAB/Simulink. Comparative analyses are conducted to assess the effectiveness of various MPPT algorithms in terms of energy yield, grid stability, and power quality enhancement.

The findings demonstrate that the integration of optimized MPPT algorithms not only enhances the overall energy conversion efficiency of RES but also contributes significantly to maintaining grid stability and improving power quality. Practical implications and recommendations for future research are discussed based on the outcomes of this study.

Keywords: Renewable Energy,Distributed Generation System,Power Quality Improvement,Grid Integration,MATLAB
Simulation.

I. INTRODUCTION

An increasing number of distributed generators based on renewable energy sources (RES) are being connected to the utility grid due to factors such as rising power consumption, technological advancements, and environmental concerns. Power electronics and digital control technologies are developing at a rapid pace, opening up additional options and improving flexibility for integrating different renewable energy sources into traditional power systems. One alternative that is gaining traction is distributed generation (DG), and other energy sources like photovoltaic, wind, fuel cells, etc., will probably play a bigger part in supplying the world's growing energy needs.

Serious issues with power quality (PQ) in the network are caused by harmonics and the reactive power requirements of non-linear loads. In order to account for harmonics and reactive power of non-linear loads, a number of active power filter (APF) topologies have been developed . Even for extremely non-linear loads, the shunt active power filter (SAPF), which is based on a voltage source inverter (VSI) that is current regulated and pulse width modulated (PWM), is the most effective topology . Different time-domain techniques based on synchronous reference frame (d-q) theory, instantaneous reactive

power (p-q) theory, and various frequency-domain techniques based on Fourier transform additionally For reference signal estimation, instantaneous active-reactive current (id-iq) theory has been devised . The implementation of these control mechanisms is difficult due to the enormous number of transformations required.

The study proposes a single-stage, three-phase, RES-based distributed generation system with APF capability, with the goals of lowering costs and boosting efficiency. The DC-link of the grid-interfacing inverter is connected to the DG source in the proposed DG system. The inverter is actively managed in the suggested method so that it provides the grid with active power from the DG. Even in the case of distorted supply voltage conditions, the suggested approach compensates for harmonics and imbalance if the load connected at the point of common coupling (PCC) is non-linear, unbalanced, or both. Thus, in addition to the active power injection from the RES, the grid-interfacing inverter is successfully used to correct the load reactive power, current imbalance, and current harmonics.

II. THE PROPOSED RENEWABLE ENERGY-BASED DISTRIBUTED GENERATION SYSTEM

The circuit for the suggested DG system is seen in Figure 1 and consists of a RES coupled to a CC-VSI for grid interface through an energy storage DC-link.

capacitor, DC. The AC side of the VSI is connected to an inductive filter. Before the system is connected to the PCC, the voltage level is raised using a step-up transformer.

At the PCC, there is a non-linear load linked to an uncontrolled diode rectifier. The purpose of the inverter control is to control the flow of DG power to the PCC and to correct for load current harmonics and load power factor.

III. GRID-INTERFACING INVERTER DESIGN AND CONTROL CIRCUIT ANALYSIS

Assuming that the load current and PCC voltage are composed of a set of harmonic components n, where n {1, 2… N}, the load current vector IL(t) and PCC voltage vector V (t) can be represented as follows:
Grid Voltage Equation:

Vgrid=Vmsin(ωt)
Inverter Output Current Equation:
Iout=Im· sin(ωt+ϕ) Where:
Im is the peak value of the inverter output current,
ϕ is the phase angle between the grid voltage and the inverter output current.
Load Current Equation:
Iload=Iload m· sin(ωt+θ) Where:
Iload m is the peak value of the load current,
Iout=ZVgrid· cos(θtotal)
θtotal=ϕ+θ
Iout=ZVgrid· cos(ϕ+θ)· sin(ωt)
Unit current vectors (usa, usb, and usc) produced from detected source voltage and the required peak value are used to compute the reference instantaneous source currents (i*, i*, and i*).

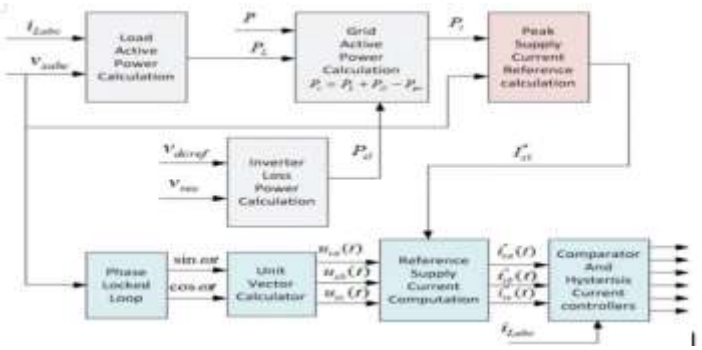

Figure 1: A distributed generation system based on renewable energy.

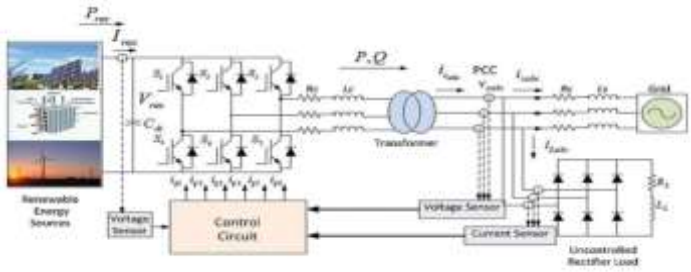

Figure 2: The grid-interfacing inverter's control circuit.

Using a phase-locked loop, the instantaneous source voltage of any one phase is used to generate the unit sine vectors. The sine template units are stated as follows:

□ica □ i* □ i

□icb □ i* □ I □icc □ i* □ I

IV. SIMULATION AND EXPERIMENTAL RESULTS

The simulation study is carried out in MATLAB where, u_1 □t□ □ sin□ t and u_2 □t□ □ cos□ t. The reference inverter currents are computed by taking the difference between instantaneous source reference currents and sensed load currents.

Simulink to verify the proposed control algorithm to achieve multi-objectives of PQ enhancement and RES power injection to the grid. The main aim of the proposed approach is to regulate the power at PCC

i^* (t)$_{ca}$□ i^* (t)$_{sa}$ □ i_{La}

i^* (t) □i^* (t) □i

There are two distinct modes of operation:

(1) PQ enhancement and RES power injection simultaneously, P_{res} □ 0 and

Cb sb Lb

i^* (t) i^* (t) *i*

(2) Only PQ enhancement mode, P_{res} □ 0. Table 1 shows the parameters used for circuit simulation.

The hysteresis current controller, which controls the PWM inverter's duty cycle, receives the error (Icica, Iicb, and Iicc) between the reference and real inverter currents.

i_{ca} □ i^* □ *i*

in two different modes of operation

(1) Simultaneous PQ enhancement and RES power injection, P_{res} □ 0 and

cb sb Lb

i^* (t) □i^* (t) □i

(2) Only PQ enhancement mode, P_{res} □ 0. Table 1 shows the parameters used for circuit simulation.

The error (□i_{ca}, □i_{cb}, □i_{cc}) between the reference inverter current and the actual inverter current are given to hysteresis current controller which regulates the duty cycle of the PWM inverter.□i_{ca} □ i^* □ *i*

(A.) Mode 1 Operation: Concurrent Power Quality Improvement Using RES Power Injection

The PCC is receiving power from RES in this mode of operation. As a result, in this instance, the grid-interfacing inverter is used in tandem to increase PCC's PQ and inject electricity generated from RES. At PCC, there is a series resistive-inductive, non-linear load coupled to an i* i⁄ic uncontrolled diode-rectifier.

The RES supply active and reactive power to local loads as per the load requirement, with the remaining active power being added to the grid. By adding a fifth harmonic voltage source of 250 Hz in series with a 50 Hz source, the grid voltage is assumed to be non-sinusoidal with a THD of 14.94%. As a result, the grid voltage harmonics have a greater impact on the grid current with higher THD levels. At t ⁉ 0.1 s, the inverter that connects the RES to the grid is turned on. As a result, the inverter begins injecting active power produced by the DG source at t ⩾ 0.1 s. The grid, load, and DG exchange active and reactive powers as shown in Figure 3a: the reactive powers are Qgrid, Qload, and Qdg, and the active powers are Pgrid, Pload, and Pdg.

The complete load power demand, including active, reactive, and harmonic load power, is met by the grid-connected inverter, which also feeds the extra active power into the system. Between periods t = 4.0 s and t = 4.2 s, there is a non-linear load variation, and between times t = 4.6 s and t = 4.8 s, there is a load imbalance. The RES output voltage Vres, output current Ires, and output power Pres are displayed in Figure 3b.

Table 1: Circuit simulation parameters
Values for parameters
Grid frequency and voltage Vs=440V (PHrms), 50 Hz
Grid resistance in phases, Rs = 0.1 Ω
Ls=0.15 mH/phase is the grid inductance.
Inductance of the filter Lc=5 mH/phase

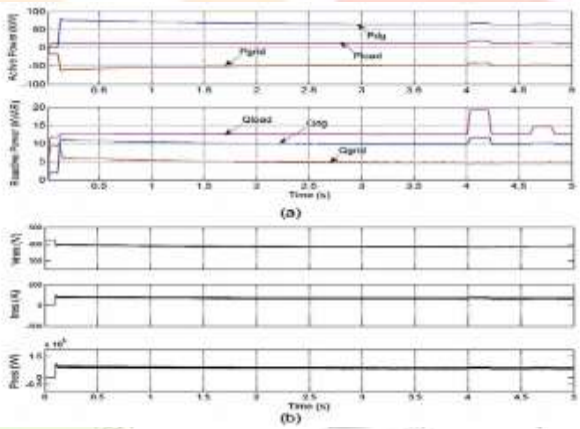

Figure 3: Mode 1 operation: PQ enhancement with RES power injection (a) Grid, load, and DG active powers (Pgrid, Pload, and Pdg) and reactive powers (Qgrid, Qload, and Qdg); (b) RES output voltage Vres, output current Ires, and output power Pres.

Initialization

Figure 4a shows the values of the PCC voltage Vs, grid current Is, load current IL, and inverter output current Ic for the times t = 0 to t = 0.25 s, or during start-up. The figure shows that the load current has a THD of 21.88% and the PCC voltage has a THD of 14.94%, both of which are extremely distorted. Grid current and three-phase PCC voltage are displayed together in Figure 4b. The grid first supplies the reactive power needed by the load connected at PCC; as a result, the voltage and current at PCC are out of phase. When the DG is turned on, the grid current and PCC voltage phase shift by 180 degrees at t 0.1 s, Start proposes feeding the grid with the extra power from DG at a power factor of unity. In addition, the grid current takes on a completely sinusoidal form. The grid current has a THD of 19.53% before correction and a THD of 4.05% after compensation with PCC load current THD of 21.88%, given a supply voltage distortion of 14.94%. When the RES is turned on, the power factor increases to 0.999.

Non-linear Variation in Load

Because non-linear loads fluctuate over time, it is necessary to examine the system's dynamic performance when non-linear load varies. The weight is made up of a resistor (RL) of 20 ″″ in series with an inductor (LL) of 10 mH after a three-phase diode rectifier. At t = 4.0 s, another R-L segment consisting of R = 20 ″″ and L = 5 mH is added to the current load, and it is removed at t = 4.2 s. As a result, the non-linear load current rises to 48.87 A at time t = 4.0 s and falls to 31.77 A at time t = 4.2 s. Figure 5 displays the PCC voltage Vs, supply current Is, variable load currents IL, and compensating current Ic for times t 3.95 s to t › 4.25 s. The outcomes validate the control's good dynamic performance for sudden changes in non-linear load.

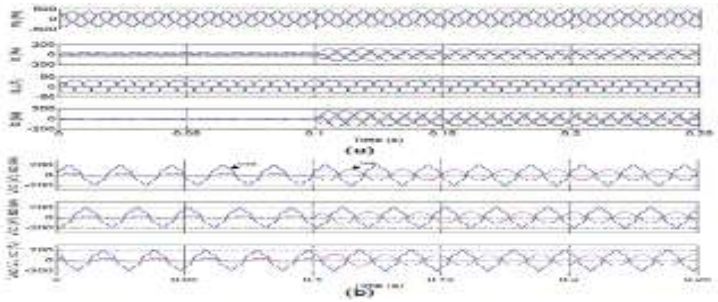

Figure 4: (a) Response of the system during startup in Mode 1: PCC voltage Vs, grid current Is, load current IL, and inverter terminal output current Ic with distorted grid voltage and non-linear load at PCC, the inverter switched on at t = 0.1 s; (b) Grid current and PCC voltage simultaneously for phase a, b and c.

Grid current THD drops from 19.53% before compensation to 7.09% after it is compensated, with load current THD of 15.00% and supply voltage distortion of 14.94%, while PCC load current increases.

Disproportionate Non-linear Load

An unbalanced non-linear load, whose imbalance, harmonics, and reactive power need to be compensated, is connected at PCC in order to confirm the compensation of non-active load currents. First, a three-phase diode rectifier makes up the load. Next, an inductor (LL) of 10 mH is connected in series with a resistor (RL) of 20 ″″. At time t = 4.6 s, a single-phase diode rectifier is connected to the PCC between phase a and phase b, and it is withdrawn at time t = 4.8 s. This is followed by a resistor R = 75 ∪. Figure 6 displays the PCC voltage Vs, supply current Is, imbalanced three-phase load current IL, and inverter output current Ic. Evidently,

At PCC, even with an uneven load, the supply currents are balanced. As a result, the suggested control can concurrently compensate for the reactive and harmonic load current components and balance the line currents. Between time t = 4.6 s and time t = 4.8 s, the THDs of the grid current are 5.78%, 5.72%, and 5.64% for phase a, b, and c, respectively, whereas the THDs of the load current are 20.34%, 18.28%, and 22.76% for each of the three phases.

The load power factor for phases a, b, and c is displayed in Figure 4a and ranges from 0.898 to 0.947. After turning on the DG, Figure 4b displays the source power factor for phases a, b, and c, which is unity negative.

(B.) Mode 2 Operation : Power quality Enhancement

There is no power generation from the DG source when operating in this mode. As a result, the grid-interfacing inverter is using a SAPF mode. While the inverter supplies the majority of the load's reactive and harmonic power, in the SAPF mode of operation, the inverter uses a tiny amount of active power from the grid to offset its losses and maintain the DC-link voltage. At time t ⁉ 0.1 s, the inverter is turned on. Figure 8 displays the reactive powers Qgrid, Qload, and Qinv, and the grid, load, and inverter active powers Pgrid, Pload, and Pinv, respectively. The inverter connects to the grid gives all of the load power that is reactive and harmonic, while the grid supplies the load power that is active. Between intervals t = 1.5 s and t = 1.7 s, there is a non-linear load variation, and between times t = 2 s and t = 2.2 s, there is a load imbalance.

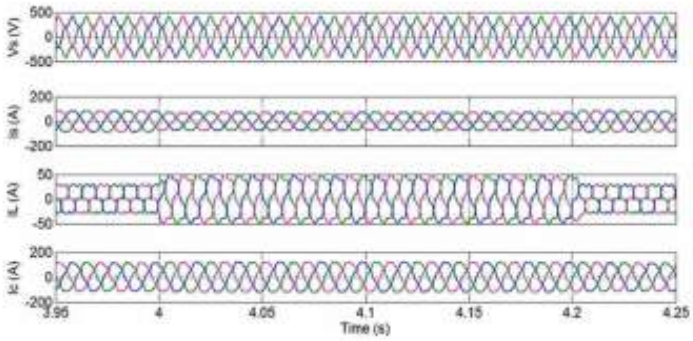

Figure 5: Response of the system to non-linear load variation in Mode 1: PCC voltage Vs, grid current Is, load current IL, and inverter terminal output current Ic with non-linear load variation at the PCC at time t = 4 s and t = 4.2 s.

Initialization

Figure 5. a displays the PCC voltage Vs, DC-link voltage Vdc, load current IL, inverter output current Ic, and grid current Is during the time interval t 0 to t 0.35 s. The three-phase grid's voltage and current are displayed simultaneously in Figure 6b. At first, the reactive power requirement of the grid provides the load linked at PCC, the grid's voltage and current are out of phase. Phase alignment between grid current and PCC voltage occurs at t 0.1s, when the inverter is turned on. In addition, the grid current exhibits perfect sinusoidal behavior, and the capacitor voltage stabilizes in a matter of cycles. With a supply voltage distortion of 14.94%, the grid current has a THD of 19.53% prior to compensation, 0.87% with compensation, and a THD of 21.88% with the PCC load current. After adjustment, the input power factor was increased to 0.999.

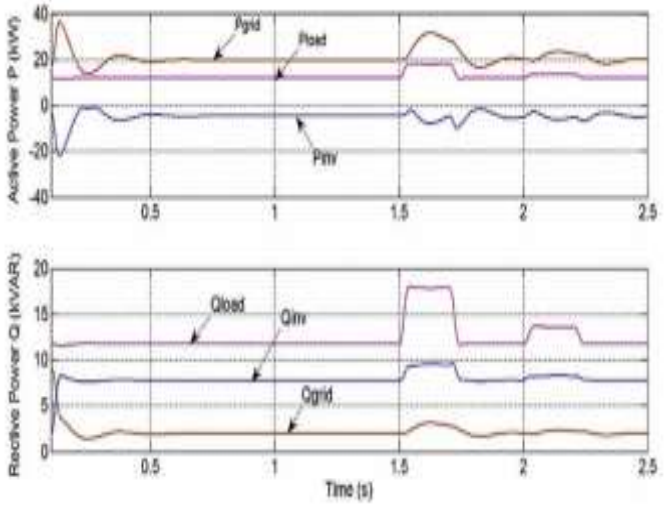

Figure 6: Mode 2 operation: Power quality enhancement, Grid, load, and inverter active powers (Pgrid, Pload, and Pinv) and reactive powers (Qgrid, Qload, and Qinv).

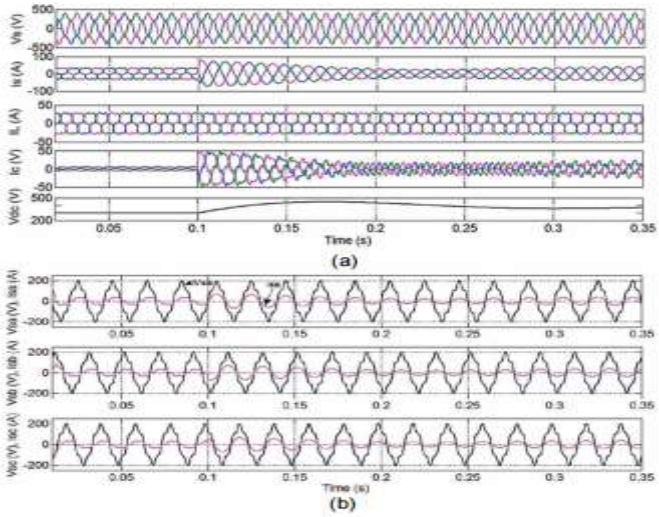

Figure 7: (a) Response of the system during start-up in Mode 2: PCC voltage Vs, grid current Is, load current IL, inverter compensating current Ic, and DC-link voltage Vdc with(a) Non-linear load and distorted

grid voltage at PCC, with the inverter turning on at t = 0.1 s. (b)Grid current and distorted grid voltage for phases a, b, and c concurrently.

Non-Linear variation in Load

At intervals t = 1.5 s and t = 1.7 s, Figure 10 displays the PCC voltage Vs, supply current Is, load current IL, compensating current Ic, and DC-link voltage Vdc for non-linear load changes. A three-phase diode rectifier is the first component of the load, and it is followed by an inductor (LL) of 10 mH in series with a resistor (RL) of 20 ″″. At t = 1.5 s, a second R-L segment consisting of R = 20 ″″ and L = 5 mH is added to the current load, and it is removed at t = 1.7 s. As a result, the non-linear load current rises to 47.08 A at time t = 1.5 s and falls to 30.67 A at time t = 1.7 s.

The outcomes validate the SAPF's strong dynamic performance for quick changes in non-linear load. Depending on how much the load current changes,

During the transient period, the capacitor voltage absorbs or releases energy by increasing or decreasing from the reference value. The steady-state condition is attained in a few supply cycles. The grid current changes smoothly in response to changes in the load current. Grid current THD drops from 19.53% before compensation to 0.59% after it is compensated, with load current THD of 15.17% and supply voltage distortion of 14.94%, while PCC load current increases.

Disproportionate Non-linear Load

For load imbalance from time t 2 s to t › 2.2 s, Figure 8 displays the PCC voltage V, supply current I, unbalanced threeb phase load current IL, inverter output current Ic, and DC-link voltage Vdc.

A three-phase diode rectifier, an inductor (LL 10 mH) connected in series with a resistor (RL 20) make up the non-linear load. At time t 2 s, a resistor R 75 ∟ is connected to the PCC between phase a and phase b, and at time t 2.2 s, it is withdrawn. This is a single-phase diode rectifier. The supply currents are balanced upon correction, as can be observed. As a result, the suggested control can concurrently compensate for the reactive and harmonic load current components and balance the line currents. Between time t 2 s and t 2.2s, the THDs of grid current are 0.76%, 0.79%, and 0.78% for phase a, b, and c, whereas the THDs of load current are 20.44%, 18.34%, and 22.79% for each of the three phases.

The load power factor for phases a, b, and c is displayed in Figure 7a and ranges from 0.880 to 0.968. The source power factor for phases a, b, and c is almost unity following correction, as seen in Figure 7b. A overview of the simulation findings for Mode 1 and Mode 2 operations in terms of the total harmonic distortions over various time intervals is provided in Table 2. The table shows that t1 denotes the amount of time before startup, t2 the amount of time after startup, t3 the amount of time for non-linear load variation, and t4 the amount of time for load imbalance.

V. EXPEREMENTAL VERIFICATION

An experimental prototype has been built for the PQ enhancement mode of operation, which is when the grid interfacing inverter is the only device used as an APF to improve the PQ at the PCC and there is no power supply from the DG. Using the TMS320F2812 fixed point digital signal processor, the suggested control method is put into practice. Table 3 lists the parameter values that were used in the experiments.The controller's performance is verified using non-linear loads and non-sinusoidal source voltages. Another non-linear load with a large series impedance is connected to the PCC in order to obtain distorted voltage, which has a 7.5% THD. In this instance, the source voltage, load current, compensated source current, and inverter compensating current waveforms are displayed for phase an in Figure 7a. and compensatory current for the inverter. Following compensation, source currents are discovered to be fully sinusoidal in shape and in phase with the corresponding source voltages. This guarantees reactive power and harmonic adjustment under non-sinusoidal source voltage conditions. Figure 7c shows the results of the FFT for the source voltage, load current, and phase-a compensating source current. The compensated source current has a THD of 3.4%, while the load current has a THD of 24.5%.

Table 2: Summary of simulation results for mode 1 and mode 2 operations

Phase		Mode 1 operation (P_{res}>0)				Mode 2 operation (P_{res}>0)			
		t_1	t_2	t_3	t_4	t_1	t_2	t_3	t_4
THD of V_S (%)	a	14.94 14.57	14.55	14.57	14.94 15.10	15.07	15.15		
	b	14.94 14.58	14.55	14.57	14.94 15.10	15.07	15.15		
	c	14.94 14.57	14.56	14.57	14.94 15.10	15.07	15.15		
THD of I_L (%)	a	21.88 15.00	22.30	20.34	21.88 20.44	22.30	15.17		
	b	21.88 14.99	22.30	18.28	21.88 18.34	22.30	15.16		
	c	21.89 14.99	22.31	22.76	21.89 22.79	22.31	15.17		
THD of I_S (%)	a	19.53 5.09	4.05	5.78	19.53 1.76	1.87	1.60		
	b	19.53 6 .99	4.13	5.72	19.53 1.79	1.86	1.82		
	c	19.53 7.29	4.02	5.64	19.53 1.78	1.91	1.81		

THD – Total harmonic distortion

Table 3: Parameters used for experimentation

Parameters	Values
Source voltage and frequency	V_S=50V rms, 50 Hz Source inductance L_S=0.15 mH
Filter inductance	L_C=2.75 mH
DC-link capacitance	C_{dc}=1500 µF
DC-link voltage reference	V_{dcref}=150 V

DC – Direct current

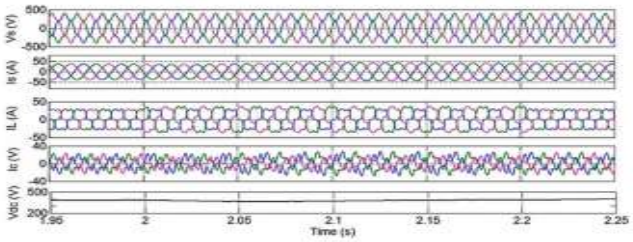

Figure 8: Response of the system to load imbalance in Mode 2: PCC voltage Vs, grid current Is, load current IL, inverter compensating current Ic, and DC-link voltage Vdc to unbalanced non-linear load at the PCC from time t = 2 s to t = 2.2

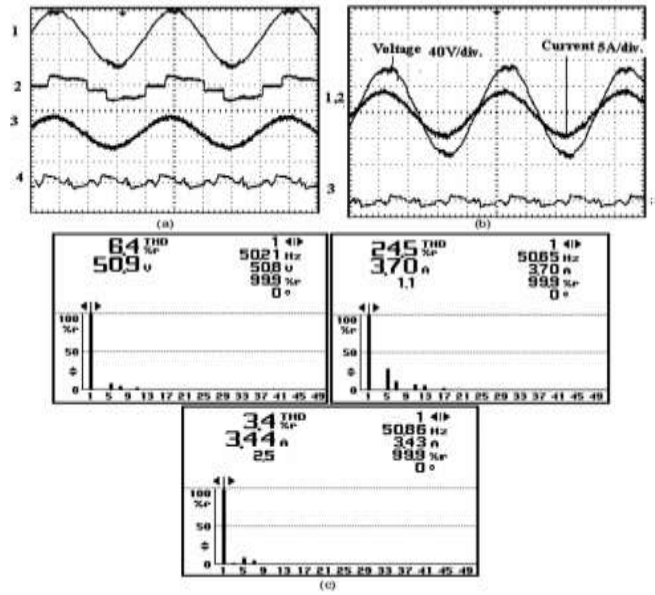

Figure 9: (a) 1 - Source voltage (75 V/div), 2 - Load current (10 A/div), 3-Source current (5 A/div), 4 - Inverter compensating current (5 A/div), (b) 1, 2 - Source voltage and source current together, 3 - Inverter compensating current, (c) THDs of source voltage, load current and compensated source current.

VI. CONCLUSION

In order to enhance the performance of an existing DG grid-interfacing inverter, this article has proposed a novel control technique. quality of electricity at PCC without interfering with real power transfer's regular operations. By using the proposed approach's grid-interfacing inverter to inject real power generated from RES into the grid and/or act as a shunt APF, extra power conditioning equipment is not required to increase the quality of power at PCC. Due to an unbalanced non-linear load connected to the PCC, the current unbalance, current harmonics, and reactive power of the load are successfully corrected so that the grid side current is balanced sinusoidal at unity power factor. The suggested method has been validated by DSP-based experimental findings and simulation in MATLAB/Simulink.

REFRENCES

[1.] IEEE Transactions on Power Electronics, Vol. 19, no. 5, pp. 1184–94, 2004; F. Blaabjerg, Z. Chen, and S. B. Kjaer, "Power electronics as efficient interface in dispersed power generation systems."
[2.] W Kramer, S. Chakraborty, B. Kroposki, and H. Thomas, "Part 1: Systems and Topologies: Advanced Power Electronic Interfaces for Distributed Energy Systems," Technical Report NREL/TP-581-42672, 2008.
[3.] "A new control approach to three-phase active filter for harmonics and reactive power compensation," B. Singh, K. Al-Haddad, and A. Chandra, IEEE Transactions on Power Systems, Vol. 13, no. 1, pp. 133–8, 1998.
[4.] An enhanced control method of shunt active filter for voltage regulation, harmonic removal, power-factor correction, and balancing of nonlinear loads was published in IEEE Transactions on Power Electronics, Vol. 15, no. 3, pp. 495–507, 2000 by A Chandra, B Singh, B N Singh, and K Al-Haddad.
[5.] "A Control Algorithm for Compensation of Customer-Generated Harmonics and Reactive Power," S. K. Jain, P. Agarwal, and H. O. Gupta, IEEE Transactions on Power Delivery, Vol. 19, no. 1, pp. 357–66, 2004.
[6.] The article "Harmonic and reactive power compensation with shunt active power filter under non-ideal mains voltage condition" was published in the Journal of Electric Power Systems Research in 2005. It was authored by M. Kale and E. Ozdemir.
[7.] "A control algorithm for single-phase active power filter under non-stiff voltage source," L P Kunjumuhammed and M K Mishra, IEEE Transactions on Power Electronics, Vol. 21, no. 3, pp. 822–825, 2006.
[8.] "PI controlled three-phase shunt active power filter for power quality improvement," A. Chaoui, J. P. Gaubert, F. Krim, and G. Champenois, International Journal of Electric Power Components and Systems, Vol. 35, no. 12, pp. 1331–44, 2007.

[9.]Journal of Electric Power Components and Systems, Vol. 38, no. 8, pp. 937–59, 2010.
[10.] "Experimental Design of a Nonlinear Control Technique for Three-Phase Shunt Active Power Filter," IEEE Transactions on Industrial Electronics, Vol. 57, no. 10, pp. 3364–75, 2010, S. Rahmani, N. Mendalek, and K. Al-Haddad.
[11.] Grid Interconnection of Renewable Energy Sources at the Distribution Level With Power-Quality Improvement Features, by M. Singh, V. Khadkikar, A. Chandra, and R. K. Varma, IEEE Transactions on Power Delivery, Vol. 26, no. 01, pp. 307–15, 2011.
[12.] In IEEE Transactions on Industry Applications, Vol. 41, no. 4, pp. 1075–83, 2005, T Wu, H Nien, C Shen, and T Chen present "A Single-Phase Inverter System for PV Power Injection and Active Power Filtering With Nonlinear Inductor Consideration."
[13.] "Novel Concept of a PV Power Generation System Adding the Function of Shunt Active Filter," Proceedings of the IEEE Transmission and Distribution Conference, Japan, pp. 1658–63, 2002, N. G. Sung, J. D. Lee, B. T. Kim, M. Park, and I. K. Yu.